

## Two Bovine Models of Osteogenesis Imperfecta Exhibit Decreased Apatite Crystal Size

L. W. Fisher, E. D. Eanes, L. J. Denholm, B. R. Heywood, and J. D. Termine

Bone Research Branch, National Institute of Dental Research, National Institutes of Health, Bethesda, Maryland 20892 USA

**Summary.** In recent years advances have been made in detailing the changes in both collagen and noncollagenous proteins caused by a variety of mutations leading to osteogenesis imperfecta. Much less, however, is known about the mineral phase in the affected bone. In this report, we measured the crystallinity of the apatite in bovine OI bone. Line broadening of the 002 reflection (which estimates changes in the long or *c* axis of the crystals) and of the 310 reflection (which estimates changes in the thickness of the crystals) both show large decreases (30 and 35% respectively). Transmission electron micrograph measurements indicate that these changes were most probably a result of smaller crystals. No decrease in the ash weight of the bone was observed.

**Key words:** Osteogenesis imperfecta — Mineral — Bone — Apatite — Crystal.

Osteogenesis imperfecta (OI) is a heterogeneous disorder that presents bone fragility with joint laxity, blue sclerae, presenile hearing loss, and dentinogenesis imperfecta in various combinations as the clinical manifestations [1]. Many cases are spontaneous mutations although OI may be inherited as either autosomal recessive or dominant traits [1]. The extracellular matrix of OI has been studied intensely in recent years. Many cases have been documented that involve collagen mutations [2–5], including mutations in the propeptide regions [6]. However, in the majority of OI cases, primary defects in the collagen structure have not been found

[7] although whether this is due to the difficulty in finding a small defect in the large collagen gene or, in some cases, to other genetic defects is unknown. In some cases noncollagenous proteins have been implicated as useful biochemical markers in the study of OI [8–10].

Recently, two separate bovine models of OI have been discovered (BOI-Australia [11]; BOI-Texas, J. B. Cruz and K. G. Thompson, personal communication). The sires for both models were phenotypically normal bulls and one-half of their offspring were affected. The symptoms included bone fragility, joint laxity, blue sclerae, and translucent, fragile teeth. No major collagen defects have yet been found in either model. We recently surveyed the noncollagenous proteins from the bones and teeth of both models and have found that the two clinically identical models could be differentiated easily by a biochemical marker, the osteonectin content of the bone matrix. BOI-Australia had normal complement of osteonectin [12], whereas severely depleted osteonectin levels were found in the bone of the BOI-Texas calves [13].

In this paper, we report on the crystallinity of the bone mineral phase in these two models.

### Materials and Methods

Dissected neonatal diaphyseal bone (normal and affected), cleaned of adherent soft tissue, was fractured into small pieces and ground to a 100 mesh size in a Spex freeze-mill under liquid nitrogen. After lyophilization, patterns of the 002 and 310 apatite mineral diffraction peaks were obtained from the bone powders on a Rigaku X-ray diffractometer using graphite-monochromatized copper  $k_{\alpha}$  radiation ( $\lambda = 0.1540$  nm). Only these two peaks were usable for the present study. Inadequate intensity or uncorrectable interference from neighboring reflections prevented a quantitative evaluation of other peaks. A continuous scan mode was employed with all data collected on a strip chart re-

order. The 002 peaks from each sample were recorded a minimum of 5 times at an angular velocity of  $0.125^\circ/2\theta/\text{min}$  using a time constant (TC) of 10 sec. A minimum of two patterns of the corresponding 310 peaks were recorded at a scanning speed of  $0.03125^\circ/2\theta/\text{min}$  and a TC of 40 sec.

The angular width (B) of the 002 diffraction peak was measured at  $\frac{1}{2}$  the height of maximum intensity above background. The half width, B, was corrected for instrumental broadening, b, by Warren's method [14], i.e.,  $B^2 = \beta^2 + b^2$ , where  $\beta$  is the corrected peak width. Silicon powder and highly crystalline synthetic hydroxyapatite were used as reference substances in determining the value of b.

The 310 reflection was not entirely free of neighboring peak influences. The 212 peak, 40% as intense as the 310 peak and situated  $-0.62^\circ 2\theta$  away, overlapped the low angle edge of the 310 peak. To minimize the effect of this overlap, the breadth of the 310 peak was estimated using the high angle side of the peak by measuring the distance between the angular position of the peak maximum and the position at which the high angle edge was  $\frac{1}{2}$  the height of maximum intensity. The half-width was obtained by multiplying this distance by 2.

Lyophilized bone fragments were prepared for transmission electron microscopy by embedding in Spurr's low viscosity resin [15]. Ultrathin sections were cut with a diamond knife onto buffered flotation fluid to minimize demineralization, then mounted on bare copper mesh grids. Micrographs were obtained using a JEOL 100CXII electron microscope operated at 80 kV. Measurements of crystal length were made on micrographs of magnification 125,000. Individual crystals were measured in mm using a measuring magnifier (Polaron 3404).

## Results

The X-ray diffraction line breadth data are given in Table 1. Since peak broadening is related inversely to crystal size and/or perfection [14], the reciprocal of the  $\beta$  values ( $1/\beta$ ) are listed in the table in order to equate more directly the experimental data to sample crystallinity (i.e., size/perfection). The  $1/\beta$  values in each column relate to crystallinity changes along specific directions in the bone mineral apatite; the 002 column data reflect changes along the length of the crystals (which is also parallel to the c- or hexad axis), and the 310 data reflect changes in directions perpendicular to the length (i.e., width/thickness). As seen from the data, the apatite mineral crystallinity was poorer in bovine OI bones than in age-matched normal controls for each direction measured. This difference was somewhat more marked in affected Texas neonatal bones than in material obtained from affected Australian calves. The neonatal OI bone changes were also relatively isotropic with the maximum decrease in crystallinity nearly the same in width/thickness (30%) as in length (35%).

Transmission electron micrographs of both normal and OI bone sections (Fig. 1) revealed a dense lattice-work of closely packed apatite

**Table 1.** Crystallinity ( $1/\beta$ ) values from the 002 and 310 X-ray diffraction peaks of normal and OI neonatal bovine mineral apatite

Sample	$1/\beta$ (002)	$1/\beta$ (310)
BOI-T #I	$1.48 \pm .04$ SD	$0.55 \pm .05$ SD
BOI-T #II	$1.63 \pm .05$	$0.55 \pm .04$
BN-T #I	$2.27 \pm .07$	$0.79 \pm .04$
BOI-A #I	$1.74 \pm .07$	$0.57 \pm .01$
BOI-A #II	$1.84 \pm .02$	$0.68 \pm .02$
BN-A #II	$2.26 \pm .04$	$0.82 \pm .04$
BN-A #III	$2.33 \pm .04$	$0.87 \pm .02$

BOI = bovine osteogenesis imperfecta bone (neonatal); BN = bovine normal bone (neonatal); T = Texas; A = Australia

crystals. Measurements of crystal length showed that the apatites in both OI models were 29–37% smaller than the normal Australian control (Table 2). A reduction in the width/thickness of OI-affected apatite crystals was also apparent but they were too closely packed together to obtain accurate measurements in these directions.

## Discussion

Studies of disease-related crystallinity changes in bone mineral apatite are limited in number. Only two other bone pathologies involving similar mineral changes have been well documented. Slight, but statistically significant, decreases in crystallinity have been observed in equine bone tumors [16]. Although the magnitude of these decreases was considerably less than observed in the present study, they also affected all crystal dimensions. In contrast, mineral crystallinity was increased rather than decreased in fluorotic bones [16–18]. The crystallinity changes in these latter bones were also more anisotropic, affecting primarily the width and thickness of the mineral apatite, leaving the length relatively unchanged [17].

The decrease in the crystallinity of the Texas OI bone mineral occurred without any significant change in tissue ash weight (OI/normal = 1.05, ref. 13). This finding suggests that the crystallinity change was linked to a defect in crystal development rather than to crystal degradation via dissolution and removal during bone turnover. The TEM data showed further that this change was due principally to arrested crystal growth rather than to a more disordered internal structure (i.e., increased lattice strain). Small-angle X-ray scattering studies on fluorotic bone [19] showed that, in this case also, metabolic disturbances in crystallinity could

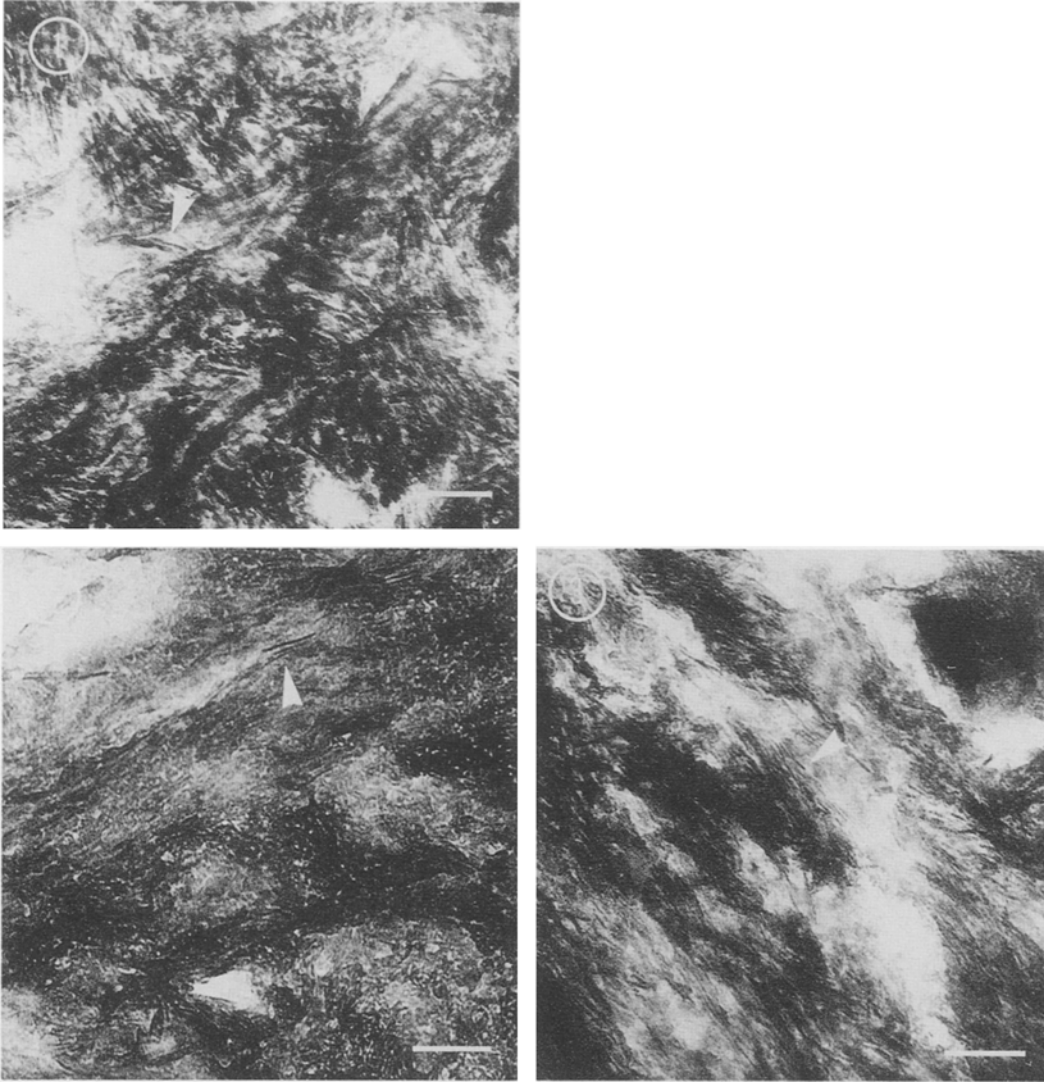


**Fig. 1.** Transmission electron micrographs of thin sections from bovine bone samples show crystallites (arrowheads). Differences in crystal size between the normal (1, Texas normal) and OI (2, BOI-A and 3, BOI-T) samples are apparent. Scale bar = 0.1  $\mu\text{m}$ .

**Table 2.** Transmission electron microscope measurement of apatite crystal length in normal and OI neonatal bovine bone

Sample	Crystal length (nm)
	Mean $\pm$ SD <sup>a</sup>
BN-A	59.0 $\pm$ 7.5
BOI-A	37.2 $\pm$ 8.7 <sup>b</sup>
BOI-T	42.1 $\pm$ 14.2 <sup>b</sup>

<sup>a</sup> Sample size = 50 measurements

<sup>b</sup> ( $P < 0.01$ )

be accounted for almost entirely by changes in crystal size.

In the Texas OI bones, the apparent decrease in crystal size in the absence of any significant change

in the total mineral mass indicates an increase in the number of apatite crystals present. It is not clear whether this increase resulted from an increase in the number of primary nucleating sites in the extracellular matrix or from a change in the rate of secondary, crystal-induced nucleation [20].

## References

1. Sillence D (1981) Osteogenesis imperfecta: an expanding panorama of variants. *Clin Orthop Rel Res* 156:11–25
2. Byers PH, Shapiro JR, Rowe D, David KE (1983) Abnormal  $\alpha$ -2 chain in type I collagen from a patient with a form of osteogenesis imperfecta. *J Clin Invest* 71:689–697
3. Chu ML, Williams CJ, Pepe G, Hirsch JC, Prockop DJ, Ramirez F (1983) Internal deletion in a collagen gene in a

- perinatal lethal form of osteogenesis imperfecta. *Nature* 304:78–80
4. de Wet WJ, Pihlajaniemi T, Myers J, Kelly TE, Prockop DJ (1983) Synthesis of a shortened pro  $\alpha 1$  (I) chain and decreased synthesis of pro  $\alpha 2$  (I) chains in a pro band and with osteogenesis imperfecta. *J Biol Chem* 258:7721–7728.
  5. Steinmann B, Rao VH, Vogel A, Bruckner P, Gitzelmann R, Byers PH, (1984) Cysteine in the triple-helical domain of one allelic product of the alpha 1 (I) gene of type I collagen produces a lethal form of osteogenesis imperfecta. *J Biol Chem* 259:11129–11138
  6. Dickson LA, Pihlajaniemi T, Deak SB, Pope MF, Nicholls AC, Prockop DJ, Myers JC (1984) Nuclease S1 mapping of a homozygous mutation in the carboxyl-propeptide coding region of the pro  $\alpha 2$  (I) collagen gene in a patient with osteogenesis imperfecta. *Proc Natl Acad Sci USA* 81:4524–4528
  7. Minor RR, Pihlajaniemi T, Prockop DJ, Denholm LJ, Wootton JAM (1984) Post-translational over-modification of type I, type III and type V collagen in bovine and human osteogenesis imperfecta. *J Cell Biol* 99:405a
  8. Takagi Y, Veis A, Sauk JJ (1983) Relation of mineralized defects in collagen matrices to noncollagenous protein components. *Clin Orthop Rel Res* 176:282–290
  9. Dickson IR, Millar EA, Veis A (1975) Evidence for abnormality of bone matrix proteins in osteogenesis imperfecta. *Lancet* 2:586–587
  10. Dickson IR, Bagga M, Paterson CR (1983) Variations in the serum concentration and urine excretion of  $\alpha_2$ HS-glycoprotein, a bone-related protein in normal individuals and in patients with osteogenesis imperfecta. *Calcif Tissue Int* 35:16–20
  11. Denholm LJ, Cole WG (1983) Heritable bone fragility, joint laxity and dysplastic dentin in Friesian calves: a bovine syndrome of osteogenesis imperfecta. *Aust Vet J* 60:9–17
  12. Fisher LW, Denholm LJ, Conn KM, Termine JD (1986) Mineralized tissue protein profiles in the Australian form of bovine osteogenesis imperfecta. *Calcif Tissue Int* 38:16–20
  13. Termine JD, Gehron Robey P, Fisher LW, Shimokawa H, Drum MA, Hawkins GR, Cruz JB, Thompson KG (1984) Osteonectin, bone proteoglycan, and phosphophoryn defects in a form of bovine osteogenesis imperfecta. *Proc Natl Acad Sci USA* 81:2213–2217
  14. Klug HP, Alexander LE (1962) *X-ray diffraction procedures*. John Wiley and Sons, New York, pp 491–538
  15. Spurr AR (1969) A low-viscosity resin embedding medium for electron microscopy. *J Ultrastruct Res* 41:115–132
  16. Shupe JL, Eanes ED, Leone NC (1981) Effect of excessive exposure to sodium fluoride on composition and crystallinity of equine bone tumors. *Am J Vet Res* 42:1040–1042
  17. Posner AS, Eanes ED, Harper RA, Zipkin I (1963) X-ray diffraction analysis of the effect of fluoride on human bone apatite. *Arch Oral Biol* 8:549–570
  18. Zipkin I, Eanes ED, Shupe JL (1964) Effect of prolonged exposure to fluoride on the ash, fluoride, citrate, and crystallinity of bovine bone. *Am J Vet Res* 25:1595–1597
  19. Eanes ED, Zipkin I, Harper RA, Posner AS (1965) Small-angle X-ray diffraction analysis of the effect of fluoride on human bone apatite. *Arch Oral Biol* 10:161–173
  20. Eanes ED, Termine JD (1983) Calcium in mineralized tissues. In: Spiro TG (ed) *Calcium in biology*. John Wiley & Sons, New York, pp 201–233

Received August 18, 1986, and in revised form November 7, 1986.